ISSN 0020-1685, Inorganic Materials, 2015, Vol. 51, No. 6, pp. 583–592. © Pleiades Publishing, Ltd., 2015.
Original Russian Text © V.K. Portnoi, A.V. Leonov, A.I. Logacheva, A.V. Logachev, A.N. Streletskii, 2015, published in Neorganicheskie Materialy, 2015, Vol. 51, No. 6, pp. 645–654.

Mechanochemical Synthesis in the Nb–Al–Si and Nb–Al–Si–C Systems

V. K. Portnoi[a], A. V. Leonov[a], A. I. Logacheva[b], A. V. Logachev[b], and A. N. Streletskii[c]

[a] *Faculty of Chemistry, Moscow State University, Moscow, 119899 Russia*

[b] *Semenov Institute of Chemical Physics, Russian Academy of Sciences, ul. Kosygina 4, Moscow, 117334 Russia*

[c] *OAO Kompozit, Pionerskaya ul. 4, Korolev, Moscow oblast, 141070 Russia*

e-mail: valeri.portnoy@gmail.com

Received April 29, 2014; in final form, November 18, 2014

Abstract—Ternary and quaternary alloys of the Nb–Al–Si and Nb–Al–Si–C systems have been produced by mechanochemical synthesis. Our results demonstrate that the milling of a 62Nb + 19Al + 19Si ternary mixture, whose composition corresponds to that of the intermetallic phase $Nb_{10}Al_3Si_3$, leads to the formation of an amorphous phase, whereas the milling of a 86Nb + 9Al + 5Si mixture, corresponding to a solid solution, results in the formation of a two-phase mixture, consisting of an amorphous phase and a nanostructured (7 nm) bcc solid solution. The addition of graphite to the starting mixtures homogenizes the MS products and reduces their particle size to ≃2 nm. The milling of a mixture with the composition $Nb_{10}Al_3Si_3C_{10}$ causes no changes in phase composition. The milling of a 78Nb + 8Al + 5Si + 9C mixture leads to the formation of an additional phase: nanoparticulate niobium carbide. Using differential thermal analysis, we have identified the sequence of transformations underlying the transition of the MS alloys to an equilibrium state. After the compaction of the MS powders by hot isostatic pressing, the samples prepared from the graphite-containing mixtures were more homogeneous in the case of both the alloys based on the intermetallic phase and the Nb-based solid solutions. The carbide nanoparticles precipitating on grain boundaries increase the hardness H_V of the alloys by almost 30%: from 12.75 to 18.13 GPa for the samples corresponding to the intermetallic phase and from 4.76 to 6.85 GPa for the samples corresponding to solid solutions.

DOI: 10.1134/S0020168515050143

INTRODUCTION

In recent years, Nb-based alloys, in particular those in the Nb–Al and Nb–Si systems, have attracted considerable attention for improving the high-temperature strength of structural materials and as an attractive alternative to high-temperature nickel alloys. As shown in a review by Svetlov [1], transition-metal silicides with the M_5Si_3 stoichiometry have high melting points in the range 2500–2800 K and low density (6.6–7.2 g/cm^3 in the Nb–Si system). Their working temperatures reach 1350°C, which is 200°C above the temperature range where single crystals of the latest generation of high-temperature nickel alloys can be employed. For the same reason, there is considerable research interest in the ternary system Nb–Si–Al [2]: the addition of aluminum to Nb–Si alloys improves their heat resistance, without significantly reducing their creep resistance [3, 4].

The mechanochemical synthesis (MS) of Nb–Si alloys has been the subject of very few studies. For example, Li et al. [5, 6] showed that milling led to amorphization of a mixture with the composition $Nb_{50}Si_{50}$ through the formation of Nb_5Si_3 and $NbSi_2$ as intermediate phases. The binary system Nb–Al also has been the subject of studies with the use of MS [7–9]. The alloy obtained by Dymek et al. [7] via attritor processing of mixtures of two compositions, Nb + 18 and 20 at %, consisted of several phases: Nb⟨Al⟩ niobium-based solid solution, two intermetallic phases Nb_3Al and Nb_2Al, and trace levels of fine-particle Al_2O_3. As shown by Rock et al. [8], a Nb + 23 at % Al alloy prepared by MS can be consolidated to 99% relative density, with its grain size remaining under 35 nm. The modification of a two-phase (Nb_2Al + Nb_3Al) alloy prepared by arc melting was reported in Ref. [9]. The composition of the alloy was modified by mechanical alloying with niobium; that is, the alloy was brought to another composition range (Nb_3Al + Nb) of the phase diagram. As shown in a study of the thermal stability of a $Nb_{68}Al_{32}$ alloy prepared by MS [10], the decomposition of this supersaturated solid solution as a result of heating to 1000°C occurs through the formation of an intermediate metastable *B*2-ordered bcc phase.

The objectives of this work were to synthesize Nb–Si–Al and Nb–Si–Al–C alloys using MS, assess their thermal stability, and analyze the microstructure of the alloys in a compact state.

Table 1. Starting-mixture compositions for the MS of the alloys

No.	Sample	Atomic percent				Weight percent			
		Nb	Al	Si	C	Nb	Al	Si	C
1	62Nb–19Al–19Si	62.5	18.75	18.75		84.90	7.40	7.70	
2	86Nb–9Al–5Si	86	9	5		95.42	2.9	1.68	
3	57Nb–17Al–17Si–9C	56.82	17.05	17.05	9.08	83.44	7.27	7.57	1.72
4	78Nb–8Al–5Si –9C	78.18	8.18	4.55	9.09	94.07	2.86	1.66	1.41

EXPERIMENTAL

We prepared starting powder mixtures of four compositions (Table 1) using extrapure-grade (99.96+%) Nb, Al, Si, and graphite powders ranging in particle size from 40 to 80 μm.

The composition of mixture *1* corresponds to the intermetallic phase $Nb_{10}Al_3Si_3$, and that of mixture *2* corresponds to the Nb-based solid solution region (the solubility limit of Al in Nb is ≃15 at % and that of Si in Nb is ≃5 at %). The compositions of mixtures *3* and *4* differ from those of mixtures *1* and *2* in that ≃9 at % graphite is added.

The mixtures were ground in a Fritsch P-7 planetary mill under an inert (argon) atmosphere. The process was run in intermittent mode for cooling and sampling. Powder samples (50–80 mg) were characterized by X-ray diffraction and differential thermal analysis (DTA). Milling was continued until no changes in X-ray diffraction patterns were detected. For all four mixtures, the longest milling time was 9 h.

X-ray diffraction patterns were collected on a DRON-3 diffractometer (CuK_α radiation, graphite monochromator). In diffraction data processing, we used the OUTSET, PHAN, and SPECTRUM programs [11]. In a number of cases, we evaluated the crystallite size using the Scherrer formula (D (nm) = $\lambda/\beta\cos\theta$, where λ (nm) is the X-ray wavelength and β is the full width at half maximum of the X-ray line used).

The thermal stability of the powders prepared by MS was assessed by DTA during heating to 1100°C at a rate of 10°C/min using a Netzsch STA 409 thermoanalytical system.[1] The powders (5-g samples) were compacted in steel capsules after electron-beam sealing under vacuum, followed by hot isostatic pressing (HIP) at a temperature of 1400°C for at least 2 h using a manostat system (OAO Kompozit).

[1] This part of the present work was carried out using equipment at the Shared Characterization Facilities Center, Moscow State University, and was supported by the RF Ministry of Education and Science (state contract no. 16.552.11.7081).

EXPERIMENTAL RESULTS

Milling of the Ternary Mixtures 62Nb–19Al–19Si and 86Nb–9Al–5Si

Figure 1 shows X-ray diffraction patterns of powder alloys obtained by milling mixtures *1* and *2* for 9 h. As a result of the milling, mixture *1* converted into an amorphous phase (in Fig. 1b, the X-ray diffraction pattern is presented together with a best fit curve, which adequately represents the measured profile). The amorphous phase emerged after milling mixture *1* for 3 h; after 9 h of milling, the content of this phase reached $Q \simeq 100\%$.

The material obtained by milling mixture *2* (Fig. 1a) consisted of two phases: a Nb⟨Al, Si⟩ solid solution (with a lattice parameter $a = 0.3297$ nm and a crystallite size $D \simeq 4$ nm) and an amorphous phase ($Q \simeq 30\%$). Estimating the amount of the amorphous phase as a function of milling time, we found that, in the case of composition *1*, the amorphous phase emerged at earlier stages of milling and more rapidly than in the case of alloy *2*.

Milling of the Carbon-Containing Mixtures

To avoid the formation of a carbide of one of the components (Nb or Si), we used a two-step milling procedure. First, mixtures *1* and *2* were milled (activated) for 7 h. Next, to the resultant powders was added 9.08 at % graphite, and mixtures *3* and *4*, containing graphite, were milled for an additional 2 h. The additional milling produced no drastic changes in the phase composition of sample *3* but further increased the width of the first line in its X-ray diffraction pattern because of the decrease in the particle size of the powder.

After milling, the X-ray diffraction pattern of mixture *4* showed additional broad lines (Fig. 2), in con-

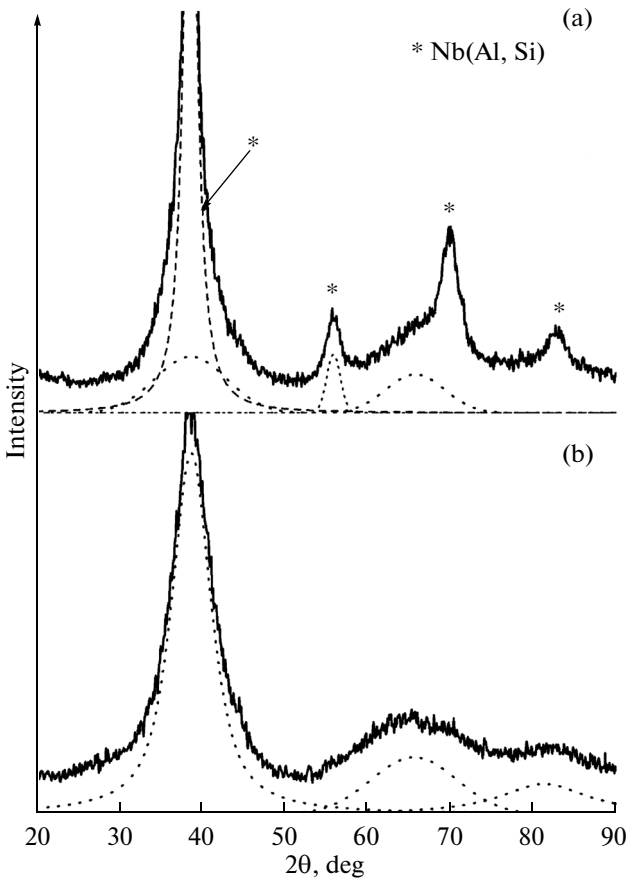

Fig. 1. X-ray diffraction patterns of MS powders after milling for 9 h: alloys with the compositions (a) 86Nb–9Al–5Si and (b) 62Nb–19Al–19Si.

trast to that of its graphite-free analogue. Those lines were tentatively attributed to the NbC carbide, which, however, was not identified with certainty, because it was probably formed in activated surface layers and consisted of small particles ($D \simeq 2$ nm). In addition to the formation of the fine-particle niobium carbide, we observed a decrease in lattice parameter to $a = 0.3290$ nm. This was due to the aluminum enrichment of the solid solution, because some of the niobium passed to the carbide.

Thermal Stability of the Powder Alloys Prepared by MS

Heating-induced transformations of the MS alloys *1* and *3*. Figure 3 shows heating curves obtained for the MS alloys *1* and *3* in a calorimeter. The differential scanning calorimetry (DSC) curve of sample *1* has one exothermic peak, at a temperature $t_{max} \simeq 850$°C, whereas the DSC curve of sample *3*, containing graphite, has a split exothermic peak, with $t_{max} \simeq 770$ and 840°C, corresponding to two processes. To identify these thermal events, the samples were characterized

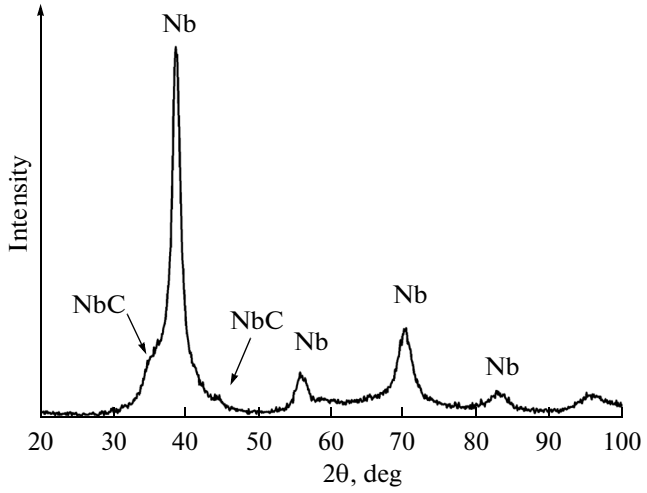

Fig. 2. X-ray diffraction pattern of the MS powder of composition *4*.

by X-ray diffraction after heating to temperatures of 1000, 1200, and 1400°C (Table 2).

After heating sample *1* to 1000°C (that is, to above the exothermic peak), only crystalline phases were detected. This demonstrates that the exothermic event is the crystallization of the amorphous phase. It is seen from Table 2 that the content of the $Nb_{10}Al_3Si_3$ (tetr) phase is ≃27 wt %. The contents of the two Nb_5Si_3 polymorphs, hexagonal and tetragonal, are 38 and 33 wt %, respectively. These phases have increased unit-cell parameters, suggesting that they contain dissolved Al. The Al solubility in Nb_5Si_3 is ≃8 at %, and dissolved Al atoms substitute for Si atoms [12].

Heating to 1200°C led to a reduction in the content of the hexagonal Nb_5Si_3 phase to 7 wt %, and tetragonal $Nb_5Si_3Al_3$ and Nb_5Si_3 became major phases. After

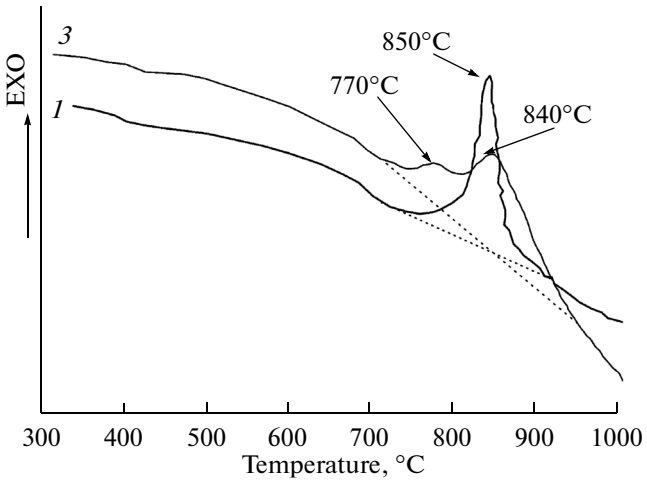

Fig. 3. DSC heating curves of the MS powders *1* (62Nb–19Al–19Si) and *3* (57Nb–17Al–17Si–9C).

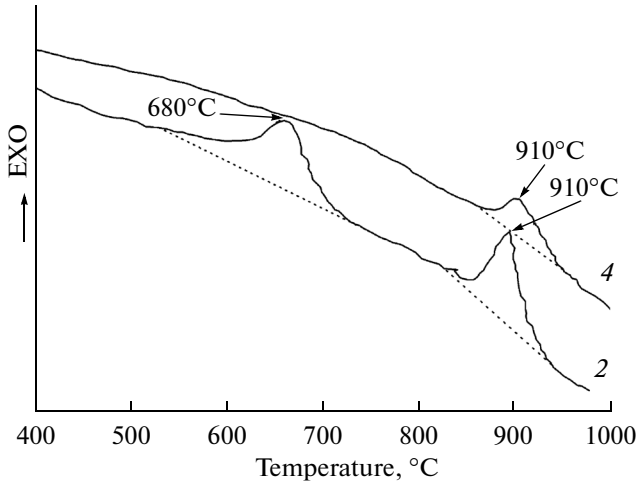

Fig. 4. DSC heating curves of the MS samples *2* (86Nb–9Al–5Si) and *4* (76Nb–9Al–5Si–10C).

HIP, (1400°C, 2-h holding), the phase composition was essentially identical to that of the starting mixture: $Nb_{10}Al_3Si_3$ (tetr) and trace levels (<5 wt %) of Nb_5Si_3 (tetr). Thus, HIP prevented the formation of Nb_5Si_3 (hex) as an intermediate phase.

Heating of sample *3* led to the formation of a new phase: a nonstoichiometric carbide of composition $NbC_{0.77}$. The formation of the carbide was responsible for the presence of the lower temperature component of the double exothermic peak in the DSC curve (Fig. 3). The high-temperature shoulder of this peak also corresponded to the crystallization of the amorphous phase (the $t_{max} = 840°C$ of this peak is close to the t_{max} of sample *1*). After heating, the major phases were the intermetallic compounds $Nb_{10}Al_3Si_3$ (hex) and Nb_5Si_3 (tetr). Thus, the carbon in the mixture stabilized the hexagonal phase.

Heating-induced transformations of the MS alloys *2* (86Nb–9Al–5Si) and *4* (76Nb–9Al–5Si–10C). Figure 4 shows DSC heating curves of the MS samples *2* and *4*. Curve *2* has two exothermic peaks, at temperatures $t_{max} = 680°C$ and $t_{max} = 910°C$, suggesting that there are two thermally activated processes: transitions to a stable state. Curve *4* shows one thermal event ($t_{max} = 910°C$).

To identify the heating-induced phase transformations, the samples were heated to 750, 1000, and 1400°C (HIP). The relevant X-ray diffraction results are presented in Table 3.

After 9 h of milling, the MS sample *2* consisted of a mixture of two phases: a Nb-based bcc solid solution and an amorphous phase (≈30%). Heating to 750°C, that is, to above the first exothermic peak, led to the crystallization of the amorphous phase and reduced the lattice parameter of the bcc solid solution from 0.3297 to 0.3287 nm. In addition, the crystallite size increased from 4 to 10 nm. The decrease in the lattice parameter of the bcc solid solution above the first exothermic peak suggests further dissolution of Si (R_{Si} = 0.118 nm) and/or Al (R_{Al} = 0.143 nm) in Nb (R_{Nb} = 0.147 nm). These elements might precipitate during the crystallization of the amorphous phase.

The second exothermic peak corresponded to partial decomposition of the solid solution. After a DTA scan to 1000°C, X-ray diffraction characterization showed the presence of a Nb-based solid solution with a lattice parameter of 0.3281 nm (Table 3) and, in addition, a small amount (3–4 wt %) of $Nb_{10}Al_3Si_3$.

HIP (1400°C, 2 h) reduced the particle size of the Nb-based solid solution (a = 0.3285 nm), which had broad diffraction lines and D = 20 nm.

The DSC curve of sample *4*, corresponding to the heating of the MS alloy *4*, had only one exothermic peak (Fig. 4). The reason for this was that, during milling of this mixture in the presence of graphite, no amorphous phase was formed.

Heating to 750°C (to the thermal event) increased the crystallite size of the Nb-based solid solution from 2 nm after milling to 8 nm after heating, without changing its lattice parameter.

Heating to 1000°C was accompanied by the decomposition of the solid solution and the precipitation of the intermetallic phase $Nb_{10}Al_3Si_3$, like in sample *2*. In addition, the cubic carbide NbC (NaCl structure) converted into the hexagonal carbide Nb_2C (NiAs structure).

Microstructure of the MS alloys *1* and *3* after HIP. Figure 5 illustrates the microstructure of alloy *1* (62Nb–19Al–19Si) after HIP. There are a large number of pores (black rounded areas 0.1 to 1.5 μm in size), which means that the heat-treatment temperature used (1400°C) was too low. Indeed, according to Abuzin et al. [13] higher HIP temperatures are needed for compacting MS alloys of the Nb–Si system. In addition to pores, two microstructural constituents can be identified in the micrograph in Fig. 5: the gray

Table 2. Phase compositions of samples *1* and *3* after heating

t, °C	Phase composition after milling and heating; *Q*, wt %	a_{meas}, nm	*D*, nm	a_{lit}, nm	Source (JCPDS)
Starting mixture *1* (62Nb + 19Al + 19Si)					
Milling	Amorphous phase; 100				
1000	$Nb_{10}Al_3Si_3$ (tetr); 27	1.0185 0.5085	27	1.016 0.5080	16-0845
	Nb_5Si_3 (hex); 38	0.7649 0.5265	35	0.7536 0.5248	65-3599
	Nb_5Si_3 (tetr); 33	0.6616 1.1919	20	0.6571 1.1889	65-2781
1200	Nb_5Si_3 (tetr); 53	0.6648 1.1930	50	0.6571 1.1889	65-2781
	$Nb_{10}Al_3Si_3$ (tetr); 40	1.018 0.5072	3	1.016 0.5080	16-0845
	Nb_5Si_3 (hex); 7	0.7657 0.5268	42	0.7536 0.5248	65-3599
1400	$Nb_{10}Al_3Si_3$ (tetr); 95	1.0207 0.5010	98	1.016 0.5080	16-0845
	Nb_2Al (tetr); 5	–	–	–	–
Starting mixture *3* (57Nb + 17Al + 17Si + 9C)					
Milling	Amorphous phase Nb (solid sol'n); <2	–	–	–	–
1200	$Nb_{10}Al_3Si_3$ (hex); 81	0.7639 0.5275	–	0.7536 0.5248	65-3599
	Nb_5Si_3 (tetr); 5	0.6583 1.1897	–	0.6571 1.1889	65-2781
	$NbC_{0.77}$; 14	0.4437	–	0.4445	89-2120
1400	$Nb_{10}Al_3Si_3$ (hex)	0.7639 0.5275	–	0.7536 0.5248	65-3599
	Nb_5Si_3 (tetr)	0.657 1.189	–	0.6571 1.1889	65-2781
	$NbC_{0.77}$	0.4437	–	0.4445	89-2120

Table 3. Phase compositions of samples *2* and *4* after heating

t, °C	Phase composition after milling and heating	a_{meas}, nm	D, nm
Starting mixture *2* (86Nb + 9Al + 5Si)			
Milling	Amorphous phase	–	–
	Nb (solid sol'n)	0.3297	4
750	Nb (solid sol'n)	0.3287	10
1000	Nb (solid sol'n)	0.3281	60
	$Nb_{10}Al_3Si_3$	–	
1400	Nb (solid sol'n)	0.3285	20
	$Nb_{10}Al_3Si_3$	–	
Starting mixture *4* (76Nb + 9Al + 5Si + 10C)			
Milling	Nb⟨Al⟩	0.3290	2
	NbC	–	–
750	Nb (solid sol'n)	0.3290	8
	NbC (NaCl structure)	0.4399	3
1000	Nb (solid sol'n)	0.3299	38
	Nb_2C	0.311 0.4953	20
	$Nb_{10}Al_3Si_3$		
1400	Nb (solid sol'n)	0.3303	15
	Nb_2C	0.311 0.4953	29
	$Nb_{10}Al_3Si_3$		30

area (major phase) and light gray areas. According to the X-ray diffraction data in Table 2, they correspond to two phases: $Nb_{10}Al_3Si_3$ (tetr) and Nb_2Al (tetr). The material was brittle: the arrows in Fig. 5 mark microcracks. The numbers in Fig. 5 mark areas and/or dots where the chemical composition was determined by X-ray microanalysis. It is worth pointing out that, at a high pore density, the accuracy of X-ray microanalysis is not very high, $\Delta C \simeq 3$ at %, but the average elemental composition is in satisfactory agreement with the starting-mixture composition, given that the material is two-phase.

Figure 6 illustrates the microstructure of sample *3* (57Nb–17Al–17Si–9C). After milling, the powder sample contained an amorphous phase and trace levels of unreacted Nb. It is seen that, after HIP, the microstructure is uniform, with nanocrystalline niobium carbide inclusions (light areas marked by arrows). The pores are considerably smaller (<0.5 μm) and are uniformly distributed over grain boundaries. The material is less brittle, without microcracks.

Microstructure of the MS alloys *2* and *4* after HIP. Figure 7 illustrates the microstructure of the MS alloy *2* (86Nb–9Al–5Si) after HIP. There are three types of areas differing in color: the light and gray areas correspond to Nb⟨Al,Si⟩ solid solutions differing in Al : Si ratio, and the black rounded dots represent pores. Given that the beam size in scanning electron microscopy (SEM) is ≃1 μm^2, the X-ray microanalysis data for points 1, 2 (gray areas), 3, and 4 (light areas) confirm the average composition of the metallic phases.

Figure 8 illustrates the microstructure of the MS alloy *4* after HIP, corresponding to a Nb-based solid solution with a grain size no greater than 1.5–2 μm. The Nb_2C carbide (marked by white arrows) and particles of the intermetallic phase $Nb_{10}Al_3Si_3$ (marked by black arrows) reside on grain boundaries and prevent grain growth during recrystallization.

Hardness of the Nb-based alloys after HIP. Table 4 lists the measured hardness values of the MS samples after HIP. It is worth pointing out that, because of the small grain size of the phases present, the indent size in microhardness measurements under a load of 2 N covers several phase fields and corresponds to hardness (H_V). It is seen from Table 4 that the hardness of sample *1*, which has the composition of the intermetallic phase $Nb_{10}Al_3Si_3$, is $H_V \simeq 12.75$ GPa. The addition of graphite to the starting mixture (sample *3*) leads to the formation of carbides and increases the hardness of the material to 18.13 GPa.

Samples *2* and *4*, where Nb-based solid solutions are major phases, have lower hardness than do the intermetallic phases, as would be expected. The addition of graphite to the starting mixture also increases the hardness of the material, by almost 30%, because of the formation of a more uniform microstructure and the precipitation of carbides nanoparticles on micrograin boundaries.

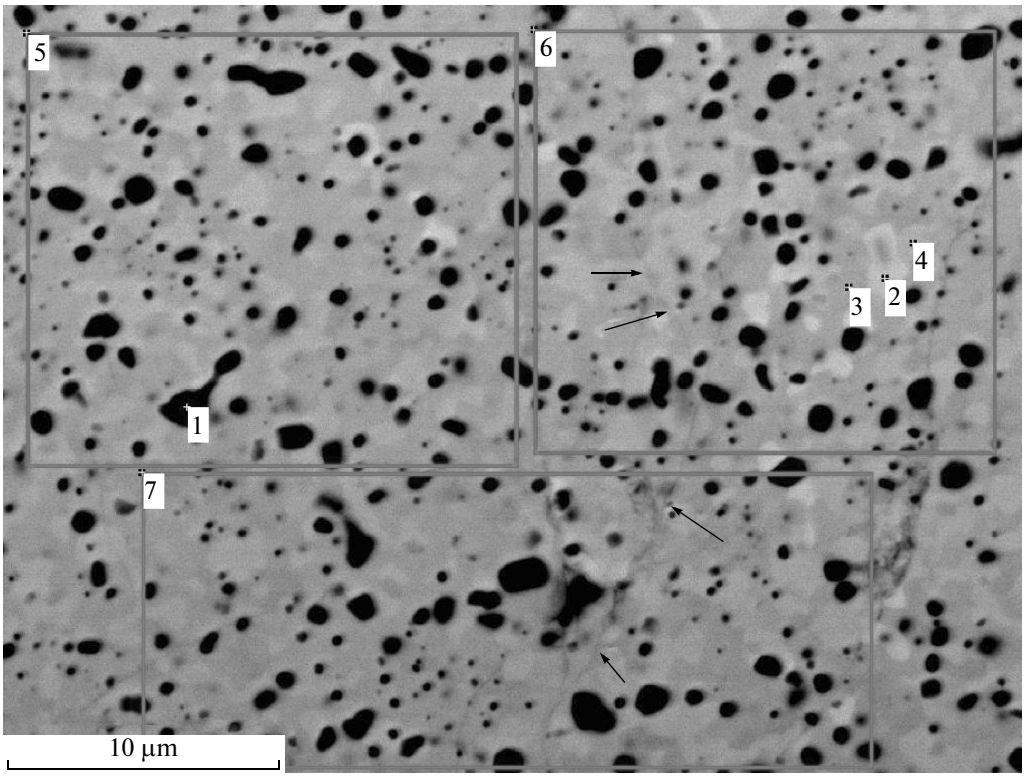

Fig. 5. Microstructure of the MS sample *1* after HIP (SEM).

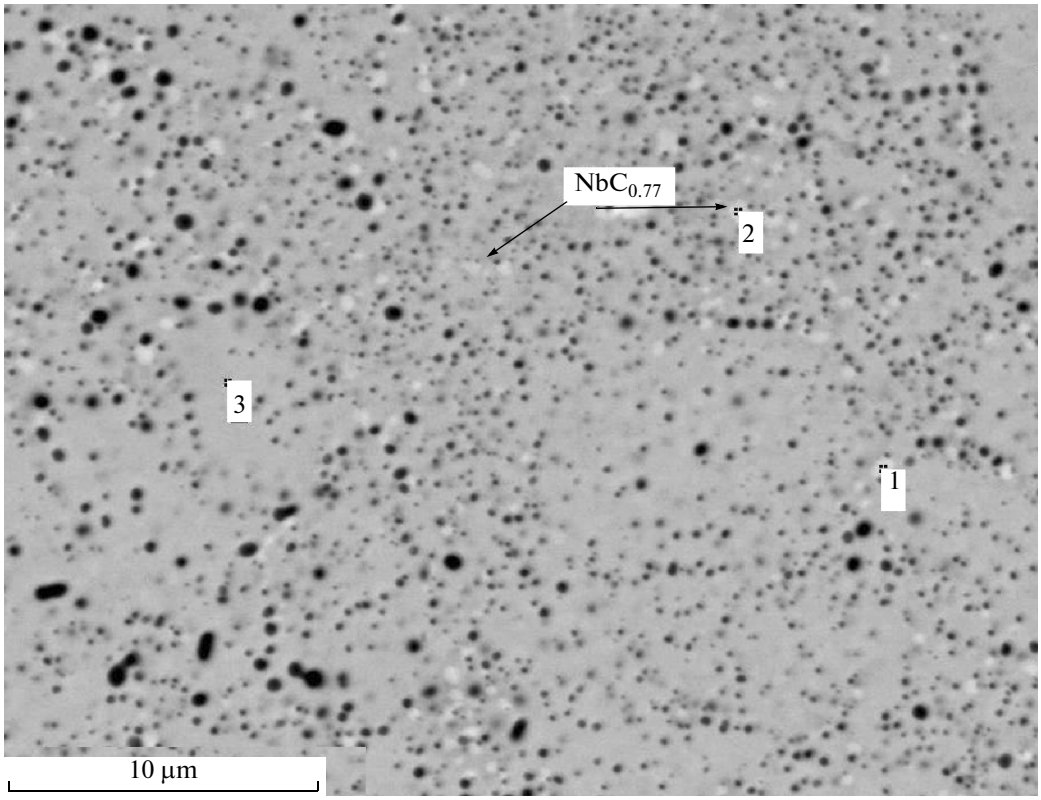

Fig. 6. Microstructure of the MS sample *3* after HIP (SEM).

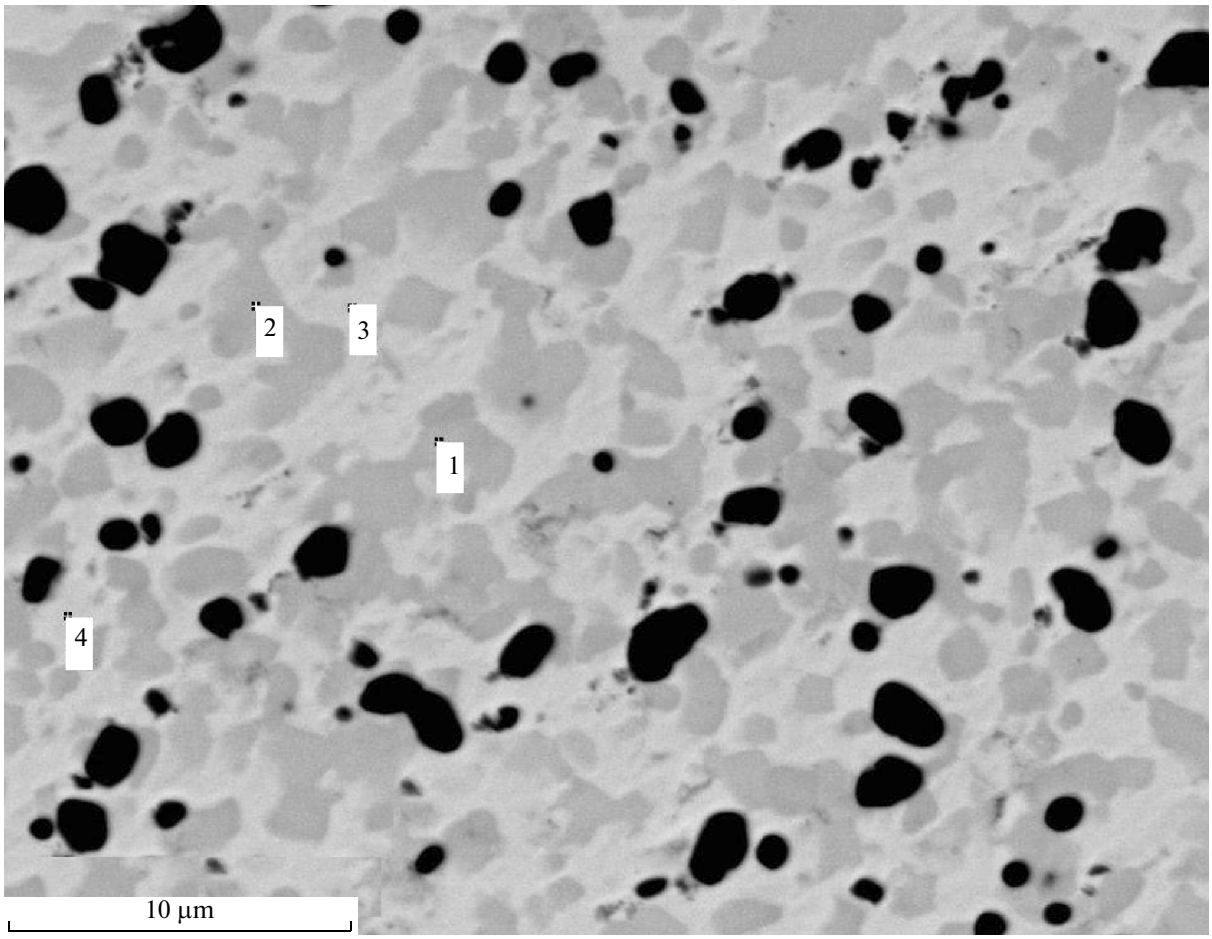

Fig. 7. Microstructure of the MS sample *2* after HIP (SEM).

DISCUSSION

It is important to note that the milling of mixtures *1* (62Nb + 19Al + 19Si) and *2* (86Nb + 9Al + 5Si) led to the formation of an amorphous phase, but through different amorphization mechanisms. In the case of mixture *1*, whose composition corresponds to the intermetallic phase, milling produced an amorphous phase without any intermediate solid solution, that is, through nucleation and growth as a result of reaction between the starting materials.

In the case of mixture *2*, whose comosition corresponds to a solid solution, the first to form was a Nb⟨Al⟩ solid solution. The decrease in the lattice parameter of Nb from $a_{Nb} = 0.3307$ nm to $a_{Nb\langle Al\rangle} = 0.3297$ nm points to Al dissolution in Nb, given the atomic radii of Nb and Al: $R_{Nb} = 0.147$ nm and $R_{Al} = 0.143$ nm. Amorphization began only after 3 h of milling, when there was no elemental Si.

In the initial stage of milling, the reaction path may be determined by pair interactions between the elements present in the mixture. According to the Nb–Al phase equilibrium diagram [14, 15], the Al solubility in Nb at 600°C is ≃7 at %. As a result of MS, it may reach 32 at % [11]. At the same time, silicon has negligible solubility in Nb and they form several intermediate

Table 4. Hardness of the HIPped Nb–Al–Si and Nb–Al–Si–C samples

Sample	*1*	*2*	*3*	*4*
Composition, at %	62Nb–19Al–19Si	86Nb–9Al–5Si	57Nb–17A–17Si–9C	78Nb–18Al–5Si–9C
H_V, GPa	12.75	4.76	18.13	6.85

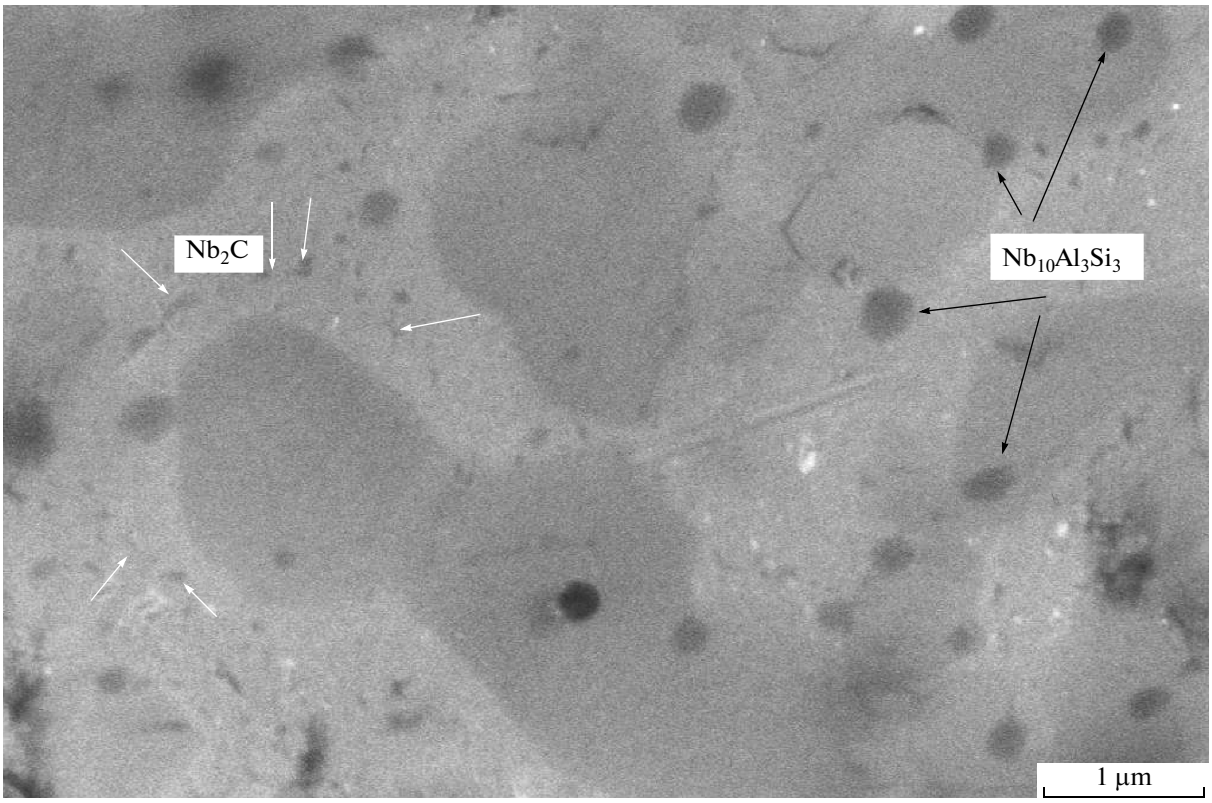

Fig. 8. Microstructure of the MS sample *4* after HIP (SEM).

phases [16]. During MS from mixtures of Nb and Si, amorphous phases form readily [6, 7]. Therefore, silicon acts as an amorphization agent in the Nb–Al–Si system: only after it disappears, which takes 5–7 h of milling, complete amorphization of the alloy occurs. It is thus clear that, in mixture *1*, interaction between Nb and Si prevails, and Al dissolves in the resulting amorphous phase. The relationship between the amounts of the amorphous phase (AP) during milling of mixtures *1* and *2* is $Q_{AP1}/Q_{AP2} \simeq 3$, which is comparable to the relationship between the amounts of Si in these mixtures.

It is important to note the good thermal stability of the amorphous phase produced by MS: its crystallization onset temperature exceeds 800°C.

Another issue to address is the effect of graphite additions on the MS process. On the one hand, the addition of graphite to preactivated mixtures (milling for 7 h) does not prevent carbide formation; on the other, it may provide additional abrasive components (carbide nanoparticles). Moreover, the presence of graphite prevents agglomeration of metallic particles [16]. This leads to further reduction in particle size and homogenization of the MS products, which in turn has a significant effect on the microstructure and hardness of the samples after compaction by HIP.

CONCLUSIONS

The present results on the MS in the Nb–Al–Si and Nb–Al–Si–C systems demonstrate that the milling of mixtures close in composition to the intermetallic phase $Nb_{10}Al_3Si_3$ leads to complete amorphization of the mixtures, without formation of an intermediate solid solution.

In the initial stage of the milling of mixtures whose composition corresponds to a niobium-based solid solution, Al dissolves in niobium to form a solid solution. The next step, is Si dissolution, resulting in the formation of an amorphous phase, whose content is ≃30%.

Using DTA and intermediate heating, we have identified the sequence of transformations underlying the transition of the MS alloys to an equilibrium state. The amorphous phase has been shown to have high thermal stability, with a crystallization onset temperature above 800°C.

Heating to 1000°C and crystallization lead to the precipitation of $Nb_{10}Al_3Si_3$ and two Nb_5Si_3 polymorphs: hexagonal and tetragonal.

The addition of graphite to the starting mixtures homogenizes the MS products and reduces their particle size to ≃2 nm. After compaction by HIP, the presence of carbon increases the hardness of the compacts owing to carbide formation.

ACKNOWLEDGMENTS

This work was supported by the Russian Foundation for Basic Research (grant no. 12-03-00227) and the Chemistry and Materials Science Division of the Russian Academy of Sciences (basic research program no. 2).

REFERENCES

1. Svetlov, I.L., High-temperature Nb–Si composites: an attractive alternative to single-crystal refractory nickel alloys, *Dvigatel'*, 2010, no. 5, pp. 71–73.
2. Zhao, J.-C., Peluso, L.A., Jackson, M.R., and Tan, L., Phase diagram of the Nb–Al–Si ternary system, *J. Alloys Compd.*, 2003, no. 360, pp. 183–188.
3. Murakami, T., Sasaki, S., Ichikawa, K., and Kitahara, A., Microstructure, mechanical properties and oxidation behavior of Nb–Si–Al and Nb–Si–N powder compacts prepared by spark plasma sintering, *Intermetallics*, 2001, vol. 9, no. 7, pp. 621–627.
4. Kashyap, S., Tiwary, C.S., and Chattopadhyay, K., Microstructure and mechanical properties of oxidation resistant cast Nb–Si–Al alloy, *Mater. Sci. Eng., A*, 2013, vol. 559, pp. 74–85.
5. Li, B., Liu, L., Ma, X., Qi, Z., and Dong, Y., Investigation of amorphization of Nb–Si alloys by mechanical alloying, *Chin. Phys. Lett.*, 1994, vol. 11, no. 11, pp. 681–684.
6. Li, B., Liu, L., Ma, X.M., and Dong, Y.D., Amorphization in Nb–Si system by mechanical alloying, *J. Alloys Compd.*, 1993, vol. 202, pp. 161–163.
7. Dymek, S., Dollar, M., and Leonard, K., Synthesis and characterization of mechanically alloyed Nb_3Al-base alloys, *Mater. Sci. Eng., A*, 1997, vols. 239–240, pp. 507–509.
8. Rock, C., Qiu, J., and Okazaki, K., Electro-discharge consolidation of nanocrystalline Nb–Al powders produced by mechanical alloying, *J. Mater. Sci.*, 1998, vol. 33, pp. 241–246.
9. Portnoy, V.K., Tret'yakov, K.V., Logacheva, A.I., Logunov, A.V., and Razumovskii, I.M., Method of mechanochemical synthesis for the production of nanocrystalline Nb–Al alloys, *Phys. Met. Metallogr.*, 2004, vol. 97, no. 2, pp. 193–198.
10. Portnoi, B.K., Leonov, A.V., Streletskii, A.N., and Tret'yakov, K.V., Heating-induced phase transformations of $Nb_{68}Al_{32}$ prepared by mechanical alloying, *Izv. Akad. Nauk, Ser. Fiz.*, 2005, vol. 69, no. 9, pp. 1342–1344.
11. Shelekhov, E.V. and Sviridova, T.A., Programs for X-ray diffraction analysis of polycrystals, *Metalloved. Term. Obrab. Met.,* 2000, no. 8, pp. 16–19.
12. Shao, G., Thermodynamic assessment of the Nb–Si–Al system, *Intermetallics*, 2004, no. 12, pp. 655–664.
13. Abuzin, Yu.A., Efimochkin, I.Yu., and Svetlov, I.L., RF Patent 2 393 060.
14. Massalski, T.B., Okamoto, H., et al., *Binary Alloy Phase Diagrams*, Materials Park: ASM International, 1990, 2nd ed.
15. Kocherzhinskiy, Yu.A., Yupko, L.M., and Shishkin, E.A., *Izv. Akad. Nauk SSSR, Met.*, 1980, no. 1, pp. 184–188.
16. Portnoi, V.K., Leonov, A.V., Logachev, A.V., Streletskii, A.N., and Popov, V.A., Mechanical alloying as method for introducing carbon in Ni_3Al intermetallide, *Phys. Met. Metallogr.*, 2012, vol. 113, no. 12, pp. 1169–1181.

Translated by O. Tsarev